A NUMERICAL STUDY OF THE FORMATION OF SUMMERTIME ARCTIC STRATUS CLOUDS

Sachio OHTA

Department of Sanitary Engineering, Faculty of Engineering, Hokkaido University, Kita-ku, Sapporo 060

Abstract: A numerical study was made on the formation of summertime arctic stratus clouds which are considered to be generated due to cooling of the warm moist air advected over the polar ice from the surrounding area of the arctic ocean. A model was constructed in which a system of equations for a steady-state planetary boundary layer on cloudy days is transformed into a one-dimensional, time-dependent system of equations by introducing the downstream derivative where the time corresponds to the travel time moving with the geostrophic wind velocity.

Eddy diffusivities which were obtained by KONDO from measurements under strongly stable conditions in the atmospheric surface layer are adopted in the calculation. Upon using the method of P_3 approximation for calculating the equation of radiative transfer, the radiative effects are incorporated into the model including scattering, absorption and emission of radiation by cloud droplets as well as absorption and emission of radiation by gaseous constituents. With this model a simulation was carried out for the U.S. standard atmosphere, Arctic, July as an initial condition. The results of calculation are as follows.

The cloud appears at a height about 70 m because of the lowering ground surface temperature. After the cloud formation, on account of intense radiative cooling near the top of the cloud the temperature decreases greatly and the condensation of water vapor is much enhanced. After 24 hours the temperature at the surface remains at a constant value of melting ice, while in the cloud it falls rapidly. Consequently, the cloud temperature becomes lower than that of the surface. This creates the transport of water vapor from the surface into the cloud and then accelerates the condensation of it. Because of intense radiative cooling, the temperature shows a sharp inversion in the upper layer of the cloud. As the radiative temperature change has a maximum cooling rate in this temperature inversion layer, the temperature in this layer falls down remarkably and more water vapor is condensed. Thus the cloud continues developing and gradually rises together with the intense inversion layer.

The calculated values of eddy diffusivity for momentum show a plausible behavior, but the values for heat, water vapor and liquid water show oversensitiveness against the slight change of stability, so that they need to be smoothed.

The simulated liquid water content is three times larger than the measured one and the cloud is not separated into two layers contrary to observation. It seems necessary to investigate more realistic values for the initial condition in order to gain much plausibly simulated results.

1. Introduction

In summer the arctic ocean is frequently covered with stratiform clouds. These cloud layers, which are called "arctic stratus", have a great influence on the structure of the atmospheric boundary layer and the heat balance in the arctic area. According to VOWINCKEL and ORVIG (1970), the mean cloud amount over the polar ocean in July is more than 90% and the frequency of stratiform clouds in summer exceeds 70%. JAYAWEERE and OHTAKE (1973, 1977) observed these stratus clouds and found that after a few days of the cloud formation there was seen a sharp temperature inversion in the top half of the cloud and then an interstice occurred and developed which led to form two cloud layers. The liquid water content was about $0.1 \sim 0.2$ g/m^3 and the cloud droplet had a modal radius of $6 \sim 7$ μm.

It was reported by JAYAWEERA (1977) that the occurrence of the stratus cloud over a region of the Beaufort Sea is largely related to the southerly component of 700 mb winds at Barrow and the dissipation or decrease of the clouds to the northerly component. From these results he concluded that arctic stratus is formed due to cooling of the warm moist air which is advected over the polar ice from the surrounding area of the arctic ocean.

Model calculation of formation and persistence of arctic stratus, which treated the stratus as an advection fog, was attempted by HERMAN and GOODY (1976). They showed the occurrence of cloud whose liquid water content was $0.1 \sim 0.2$ g/m^3 and its separation into two layers two days after the cloud formation. However, they disregarded the scattering effect of solar and thermal radiations due to cloud droplets, and did not give the values of radiative temperature change in their paper. Moreover, they assumed the initial temperatures at the roughness height $z_0 = 1$ mm to be 4°C or -3°C, while the temperature of the sea surface was supposed to remain constant at 0°C. But, in the arctic region, the surface temperature in July decreases monotonously from the surrounding coasts to the central polar ocean (VOWINCKEL and ORVIG, 1970), so that the air which advected from the coasts to the central polar ocean must have the same temperature at the roughness height as that of the surface. Namely, it is unnatural to assume the temperature discontinuity such as $3 \sim 4$°C between the roughness height and the surface.

In this work, regarding the stratus cloud as an advection fog, we simulated its formation by incorporating the radiative effects according to the method of P_3 approximation derived from TANAKA and OHTA (1981). Upon using this method of calculating the radiative transfer, the radiative effect can be estimated with a sufficient accuracy including scattering, absorption and emission of radiation by cloud droplets as well as absorption and emission of gaseous constituents. The temperature of the sea surface was assumed to decrease monotonously with proceeding of the advection, and the temperature at the roughness height was supposed to be the same as that of the surface. Moreover, as the temperature profile near the top of the cloud seems to become strongly stable, we employed the eddy diffusivities by KONDO *et al.* (1978) which were obtained by the measurement under strongly stable conditions in the atmospheric surface layer.

With this model a simulation was carried out for the U.S. standard atmosphere, Arctic, July as an initial condition.

2. Mathematical Model

We adopt the Cartesian coordinate (x, y, z), where x and y are horizontal axis and z vertical. The top of the atmospheric boundary layer z_E, the height of the constant flux layer z_C and the roughness of the sea surface z_0 are, respectively, supposed to be 2000 m, 20 m and 1 mm. If we assume that air mass, heat, water vapor and liquid water are transported horizontally by wind U, equations for the steady-state planetary boundary layer on cloudy days are given as follows,

$$U\frac{\partial U}{\partial x}=f(V-V_0)-\frac{\partial}{\partial z}(\overline{u'w'})\,, \tag{1}$$

$$U\frac{\partial V}{\partial x}=-f(U-U_0)-\frac{\partial}{\partial z}(\overline{v'w'})\,, \tag{2}$$

$$U\frac{\partial \theta_S}{\partial x}=-\frac{\partial}{\partial z}(\overline{\theta_S'w'})+\left(\frac{P_0}{P}\right)^{0.2857}\cdot\left[\frac{\partial T}{\partial t}\right]_R\,, \tag{3}$$

$$U\frac{\partial q}{\partial x}=-\frac{\partial}{\partial z}(\overline{q'w'})-\frac{C}{\rho}\,, \tag{4}$$

$$U\frac{\partial w_d}{\partial x}=-\frac{\partial}{\partial z}(\overline{w_d'w'})+v_g\frac{\partial w_d}{\partial z}+C\,, \tag{5}$$

where U and V are x- and y-components of wind velocity, U_0 and V_0 are x- and y-components of geostrophic wind velocity, q mixing ratio of water vapor, w_d the liquid water content, $[\partial T/\partial t]_R$ the radiative temperature change, P pressure, P_0 surface pressure, C rate of condensation, ρ air density and v_g terminal velocity of cloud droplets, respectively. The quantity θ_S is defined by the moist static energy h as follows,

$$h=C_p\left(\theta+\frac{L}{C_p}q\right)\equiv C_p\theta_S\,, \qquad \left(\theta_S\equiv\theta+\frac{L}{C_p}q\right)\,, \tag{6}$$

where C_p is the specific heat of air at constant pressure and L the latent heat of vaporization. The term $\overline{u'w'}$ and $\overline{v'w'}$ represent the vertical turbulent transport of x- and y-momentum, and $C_p\overline{\theta_S'w'}$, $\overline{q'w'}$ and $\overline{w_d'w'}$ represent the vertical turbulent fluxes of moist static energy, water vapor and liquid water content, respectively.

We adopt the direction of geostrophic wind as x-axis (therefore $V_0=0$). The wind velocity is denoted by a complex form as

$$\tilde{U}=U+iV, \tag{7}$$

where

$$\left.\begin{aligned} U&=U_0+u, \\ V&=v. \end{aligned}\right\} \tag{8}$$

In the atmosphere higher than a few hundred meters the wind U is nearly equal to the geostrophic wind U_0, and we pay attention to the behavior of the stratus cloud which exists at a height more than 100 m, so that we linearlize the advected terms in eqs. (1)–(5) with a constant geostrophic wind U_0. According to HERMAN and GOODY (1976), we transform these linearlized advected terms by using the down-stream derivative $\delta/\delta t$ as follows,

$$U_0\frac{\partial}{\partial x}\Big[\quad\Big]=\frac{\delta}{\delta t}\Big[\quad\Big]. \tag{9}$$

This means that eqs. (1)–(5) in (x, z) space are transformed to those in (t, z) space. The equivalent system of equations corresponding to eqs. (1)–(5) is

$$\frac{\delta u}{\delta t}=fv-\frac{\partial}{\partial z}(\overline{u'w'}), \tag{10}$$

$$\frac{\delta v}{\delta t}=-fu-\frac{\partial}{\partial z}(\overline{v'w'}), \tag{11}$$

$$\frac{\delta\theta_S}{\delta t}=-\frac{\partial}{\partial z}(\overline{\theta_S'w'})+\left[\frac{P_0}{P}\right]^{0.2857}\cdot\left[\frac{\partial T}{\partial t}\right]_R, \tag{12}$$

$$\frac{\delta q}{\delta t}=-\frac{\partial}{\partial z}(\overline{q'w'})-\frac{C}{\rho}, \tag{13}$$

$$\frac{\delta w_d}{\delta t}=-\frac{\partial}{\partial z}(\overline{w_d'w'})+v_g\frac{\partial w_d}{\partial z}+C, \tag{14}$$

which is equivalent to a one-dimensional, time-dependent system of equations, the same system as our previous simulation of the evolution of radiation fog (OHTA and TANAKA, 1981).

The vertical turbulent transport terms are replaced by the gradient of each quantity in the following flux-profile relationships,

$$\left.\begin{aligned} &\overline{u'w'}=-K_M\frac{\partial u}{\partial z}, &&\overline{v'w'}=-K_M\frac{\partial v}{\partial z}, \\ &\overline{\theta_S'w'}=-K_H\frac{\partial\theta_S}{\partial z}, &&\overline{q'w'}=-K_H\frac{\partial q}{\partial z}, \\ &\overline{w_d'w'}=-K_H\frac{\partial w_d}{\partial z}, && \end{aligned}\right\} \tag{15}$$

where K_M and K_H are the eddy diffusivities.

In the constant flux layer ($z_0 \leq z \leq z_C$), we have the system of equations as follows,

$$K_M \frac{\partial \tilde{U}}{\partial z} = \frac{\tilde{\tau}_0}{\rho}, \tag{16}$$

$$K_H \frac{\partial \theta}{\partial z} = -\frac{Q_0}{C_p \rho_0}, \tag{17}$$

$$K_H \frac{\partial q}{\partial z} = -\frac{E_0}{\rho_0}, \tag{18}$$

$$K_H \frac{\partial w_d}{\partial z} + v_g w_d = -W_0, \tag{19}$$

where $\tilde{\tau}_0$, Q_0, E_0 and W_0 are, respectively, the constant flux of momentum, heat, vapor and liquid water content, and ρ_0 is the surface air density.

The eddy diffusivities for momentum K_M, and for heat, water vapor and liquid water content K_H, are given by

$$K_M = \frac{\kappa z |\tilde{\tau}/\rho|}{\phi_M}, \qquad K_H = \frac{\kappa z |\tilde{\tau}/\rho|}{\phi_H}, \tag{20}$$

where κ is the Kármán constant ($=0.41$) and $\tilde{\tau}$ is the shear stress given by

$$\frac{\tilde{\tau}}{\rho} = K_M \frac{\partial \tilde{U}}{\partial z}. \tag{21}$$

The quantities ϕ_M and ϕ_H are respectively shear functions for momentum and for heat, water vapor and liquid water. As the temperature profile near the top of the cloud seems to become strongly stable, for the values of shear functions we adopt the experimental formula obtained by KONDO *et al.* (1978). They obtained this formula by measurement of heat and momentum transfers under strong stability in the atmospheric surface layer. For the stability parameter they used the gradient Richardson number Ri,

$$Ri = \frac{g}{\theta_v} \cdot \frac{\partial \theta / \partial z}{|\partial \tilde{U}/\partial z|^2}, \tag{22}$$

where θ_v is the virtual potential temperature.

In the case of stable conditions ($Ri \geq 0$), it becomes

$$\frac{K_H}{K_M} = \frac{\phi_M}{\phi_H} = \left\{ \begin{array}{ll} \dfrac{1}{7Ri}, & \text{for } 1 \leq Ri, \\ \dfrac{1}{6.873Ri + 1/(1+6.873Ri)}, & \text{for } 0 \leq Ri < 1, \end{array} \right\} \tag{23}$$

and

$$\phi_M = \begin{cases} 5.9498\,, & \text{for } 0.243 \leq Ri\,, \\ \dfrac{1+6.873Ri+47.238Ri^2}{1-0.127Ri-0.8729Ri^2}\,, & \text{for } 0 \leq Ri < 0.243\,. \end{cases} \tag{24}$$

In the case of unstable conditions ($Ri<0$), we adopt the experimental formula obtained by KONDO (1975) given by

$$\phi_M = \left[1 - \frac{16Ri}{1-0.01Ri}\right]^{-\frac{1}{4}}, \tag{25}$$

and

$$\phi_H = \phi_M^2\,. \tag{26}$$

3. Treatment of Radiation Processes

In this model the lower boundary is assumed to be sea surface whose heat capacity is very large or melting pack ice whose temperature is constant (0°C). Therefore, we need not consider the heat balance at the surface. What we must estimate is the radiative temperature change in the atmosphere. As the method of calculating the radiative temperature change is the same as the one in our previous papers (OHTA and TANAKA, 1981; TANAKA and OHTA, 1981), only a brief outline is described here.

In the clear atmosphere, the radiative heating due to absorption of solar radiation by gaseous constituents is so small that we can ignore this absorption effect, but the radiative cooling due to infrared radiation is not so small that we cannot neglect it. The latter is computed according to RODGERS and WALSHAW (1966). In the atmospheric window region ($8\sim 12\ \mu$m) the effect of the continuum absorption due to water vapor or dimer is taken into account by using the mean absorption coefficient in this spectral region given by

$$k = k_1 P + k_2 e\,, \tag{27}$$

where P is the atmospheric pressure and e is the partial pressure of water vapor. The values of the coefficients k_1 and k_2 are adopted as $k_1=0.1$ (cm^{2}g^{-1}atm^{-1}) and $k_2=$ 10.0 (cm^{2}g^{-1}atm^{-1}), respectively from the experimental data by BIGNELL *et al.* (1963) and BURCH (1970).

In the cloudy atmosphere, we must take into account absorption and scattering of solar radiation, and absorption, scattering and emission of thermal radiation due to cloud droplets, in addition to absoprtion and emission due to gaseous constituents. Though the radiative temperature change can be obtained by solving equations of radiative transfer containing these scattering processes, it is very time-consuming to solve these equations exactly such as matrix method or discrete ordinates method. Therefore, we adopt the method of P_3 approximation for calculating radiative transfer in the cloudy atmosphere derived by TANAKA and OHTA (1981). This method can save the computational time to a large extent, even though its accuracy is sufficient such as shown in the paper.

For the size distribution of cloud droplets, we assume the following Γ type distribution proposed by ZAKHAROVA (1973),

$$n(r)=\frac{A}{a_3}r^2e^{-\frac{2}{a}r}\ , \tag{28}$$

where $n(r)\mathrm{d}r$ is the number density of droplets between radii r and $r+\mathrm{d}r$, a is the modal radius and A is a normalization constant. According to a measurement (JAYAWEERA and OHTAKE, 1973), the value of a is employed to be 6.5 μm. By the same way of our previous paper (OHTA and TANAKA, 1981), the values of normalization constant A, the total number density of cloud droplet N and the mean terminal velocity v_g averaged over the size distribution are obtained as follows,

$$A=4.071\cdot N\,, \tag{29}$$

$$N=1.461\times 10^8\cdot w_d \quad (\mathrm{cm}^{-3})\,, \tag{30}$$

and

$$v_g=1.449 \quad (\mathrm{cm/s})\,. \tag{31}$$

In order to solve the equation of radiative transfer, we need to know the scattering properties of cloud droplets such as the scattering function, the volume extinction coefficient and the albedo for single scattering. These quantities are calculated from Mie theory for the size distribution given by eq. (28) and the complex refractive index compiled by HALE and QUERRY (1973).

In this model, from eq. (30) an increase of the liquid water content causes an increase of the total number density of cloud droplets. However, in the atmosphere, when the liquid water content increases, the total number density of cloud droplets seems to remain constant and the volume of each droplet seems to increase. If we assume that the cloud is made from monodisperse droplets, in the case of increasing the total number density the volume extinction coefficient becomes greater than in the case of increasing the volumes of droplets. Therefore, in this calculation we may overestimate the radiative effects a little. However, as we have no knowledge about the change of size distribution of cloud droplets with increase of the liquid water content, we use the fixed size distribution function given by eq. (28) for this simulation.

4. Boundary and Initial Conditions

A solar zenith angle is assumed to remain constant 74° neglecting the diurnal cycle of the solar radiation. The albedo of the sea surface is assumed to be 0.50 according to the measurement (HANSON, 1961).

As the travel time t in eqs. (10)–(14) is transformed to the travel distance x by a relation

$$x = U_0 t\,, \tag{32}$$

we, hereafter, consider the formation of stratus cloud in (t, z) space. For the numerical integration of the differential eqs. (10)–(14), we adopt an explicit, forward-time difference with a centered spatial difference scheme.

The geostrophic wind U_0 is supposed to be 7 m/s. For initial profiles of temperature and relative humidity at a height above 1 km we employ U.S. standard atmosphere, 75°N, Arctic, July (VALLEY, 1965). At the sea surface $(z=z_0)$ the initial temperature and the relative humidity are assumed to be 5°C and 100%, and those at $z_1=58.5$ m to be 278 K and 90%, respectively. Between z_0 and z_1, the initial potential temperature and the mixing ratio of water vapor are interpolated logarithmically with height. These initial profiles are shown in Figs. 2 and 3 indicated by numeral 00:00. For wind and eddy diffusivities, initial profiles are obtained by integrating eqs. (10) and (11) with eqs. (15)–(17), (20)–(26) for fixed initial profiles of the temperature and the mixing ratio until u, v, K_M and K_H converge into uniform values respectively. The surface temperature is assumed to decrease monotonously from 5°C at $t=0$ to 0°C at $t=24$ hours, and after that it remains constant at 0°C. As the surface is considered to be sea water or melting pack ice, the surface relative humidity is assumed to be 100%.

5. Results and Discussion

The numerical integration was carried out for travel time of 72 hours, which correspond to traveling over the distance of 1814 km with the moving velocity of 7 m/s.

The distribution of the liquid water content with height as a function of travel time is shown in Fig. 1. The cloud appears at about 70 m in height at 8:00 due to lowering of the sea surface temperature. It continues developing due to the lowering of the sea surface temperature and radiative cooling near the top of the cloud. At 24:00 the density of the cloud increases to 0.5 g/m^3 and the cloud rises to 200 m in height. After 24:00 the surface temperature remains constant (0°C), but on account of intense radiative cooling near the top of the cloud, the temperature of the upper region of the cloud continues decreasing, which enhances more condensation of water vapor. Thus the top of the cloud continues ascending. Finally, after 3 days we have the cloud whose top is 1400 m high and the liquid water content $0.4\sim0.6$ g/m^3.

The vertical distributions of temperature as a function of travel time are shown in Fig. 2. Until 24 hours the sea surface temperature continues decreasing. After that it remains constant. However, on account of intense radiative cooling near the top of the cloud, temperature in the upper region of the cloud continues decreasing. On the contrary, the atmosphere above the top of the cloud does not receive intense radiative cooling effect. Therefore, a sharp temperature inversion layer occurs below

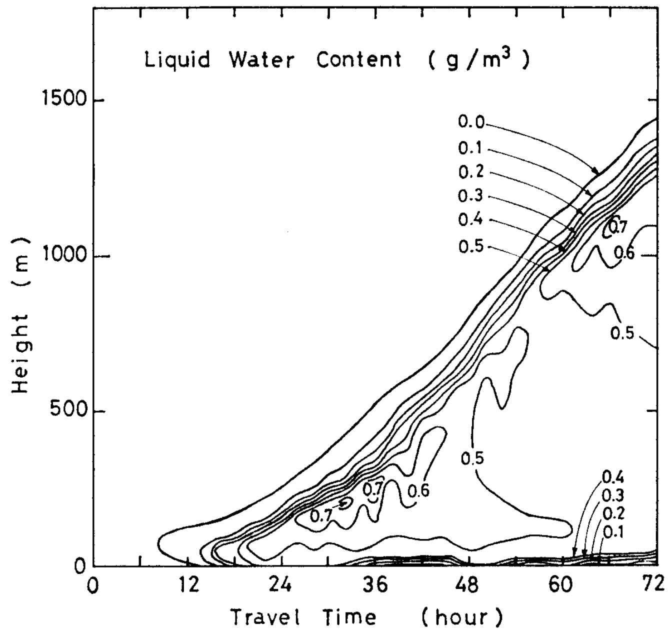

Fig. 1. Distribution of liquid water content with height as a function of travel time.

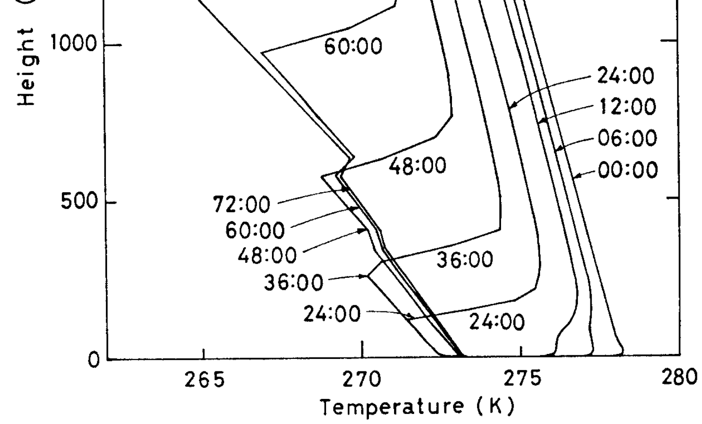

Fig. 2. Vertical distributions of temperature as a function of travel time. Numerals in the figure denote the travel time in hours.

the top of the cloud, and this inversion layer gradually rises together with the top of the cloud.

After 24 hours the surface temperature is fixed at 0°C, but the temperature in the cloud becomes lower than the surface temperature, therefore it is anticipated that water vapor is transported into the cloud from the surface of the sea. This is supported by Fig. 3 which shows the vertical distributions of the mixing ratio of water vapor as a function of travel time. As the mixing ratio at the surface is higher than that in the cloud layer, plenty of water vapor is transported into the cloud, and condenses due to intense radiative cooling. Accordingly the liquid water content increases steadily and the top of the cloud gradually rises.

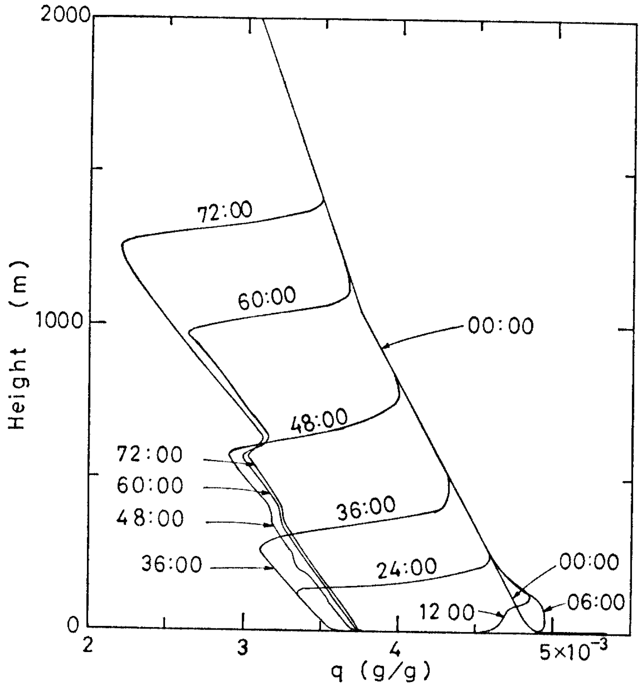

Fig. 3. The same as Fig. 2 but for mixing ratio of water vapor q.

In the previous study, if the formula of the eddy diffusivities for momentum and heat which had been obtained in the atmospheric surface layer were extrapolated to the planetary boundary layer, the simulations of the planetary boundary layer on clear days or the simulation of the evolution of radiation fog did not yield the value of diffusivity which has been obtained by field measurements. Namely, in the temperature inversion layer of above 500 m, the diffusivities decrease rapidly to zero in the simulations as in the cases given by SASAMORI (1970) with eddy diffusivities derived by YAMAMOTO and SHIMANUKI (1966), by ZUDNKOWSKI and BARR (1972) with BLACKADAR's formula (1962), and by OHTA and TANAKA (1981) with KONDO's

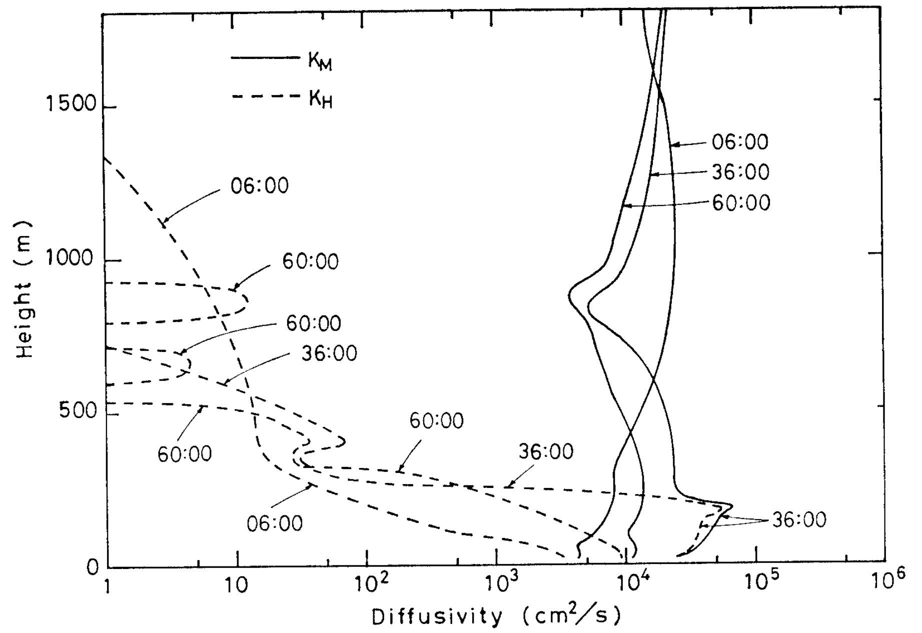

Fig. 4. The same as Fig. 2 but for eddy diffusivities for momentum K_M and for heat, water vapor and liquid water content K_H.

formula (1975). On the other hand, in the present simulation we can obtain plausible values of eddy diffusivity for momentum as shown in Fig. 4. The value of K_M ranges from 5×10^3 to 5×10^4 cm^2/s in the whole boundary layer. The value decreases slightly near the top of the cloud where the temperature shows a sharp inversion, but does not vanish to zero. While eddy diffusivity for heat, water vapor and liquid water K_H shows a sudden decrease or increase in a stable or unstable region at a few hundred meters above the ground. This shows the oversensitiveness of eq. (23) in the atmosphere above that height. Therefore, it seems necessary to smooth the calculated values of K_H when eq. (23) is applied to the planetary boundary layer.

Fig. 5 shows the vertical distributions of temperature, liquid water content, radiative temperature change due to solar radiation (SR), due to infrared radiation (IR) and total radiative temperature change (TR) at travel time of 60 hours (travel distance $x=1512$ km). The cloud has a maximum density of 0.57 g/m^3 and a minimum temperature 266.7 K at a height about 980 m, from where the temperature shows an intense inversion to the top of the cloud. The lapse rate from the surface to 980 m is $0.7\sim0.8$°C/100 m. The lapse rates at the heights of 350 m and 600 m are different from others. These peculiar lapse rates are caused by the behavior of wind profile. The wind speed has a maximum value at 350 m and a minimum one at 600 m, so that the wind shear becomes less and Ri increases greatly near there. From eq. (23), K_H decreases extremely at these heights and then the transport of heat,

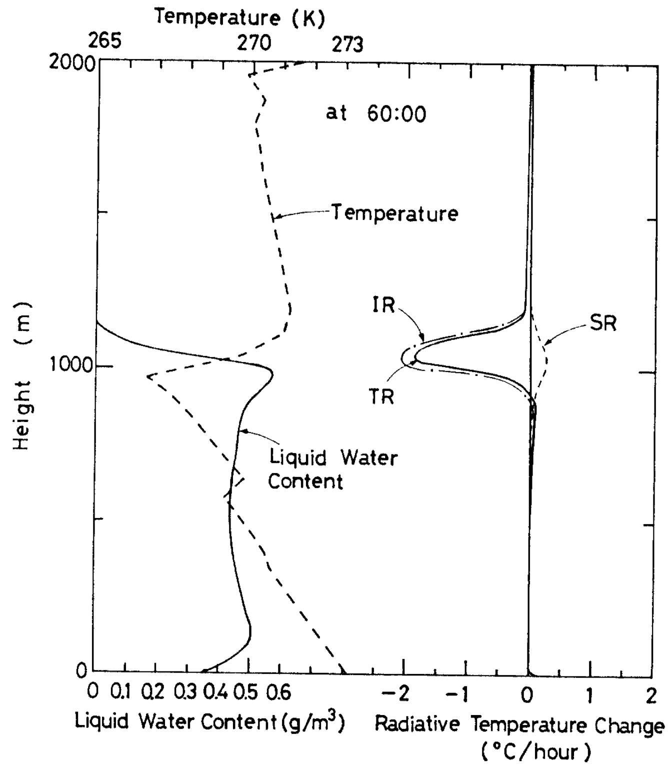

Fig. 5. Vertical distributions of temperature, liquid water content, radiative temperature change due to solar radiation (SR), due to infrared radiation (IR) and total radiative temperature change (TR) at the travel time of 60 hours (travel distance 1512 km).

water vapor and liquid water content diminishes remarkably there. On account of these effects, the lapse rates have peculiar values there.

The radiative heating rate due to absorption of solar radiation has a maximum value of 0.25°C/hour at a height of 1030 m. The radiative temperature change due to infrared radiation has a maximum cooling rate −2.10°C/hour at a height of 1030 m and a maximum heating rate 0.1°C/hour at a height of 900 m. Consequently, the total radiative temperature change has a maximum cooling rate −1.85°C/hour at 1030 m and a maximum heating rate 0.15°C/hour at 900 m. As the maximum cooling rate occurs in the intense inversion layer near the top of the cloud, the temperature in this layer goes down greatly and the condensation of water vapor is enhanced. Thus the top of the cloud rises gradually accompanied with the intense inversion layer.

According to the measurements (JAYAWEERA and OHTAKE, 1973, 1977), after a few days of the cloud formation the temperature showed a sharp inversion in the top half of the cloud, and then an interstice occurred and developed which led to form two cloud layers. The liquid water content was 0.1∼0.2 g/m^3. In this study, an intense temperature inversion layer was simulated, but the calculated liquid water content was three times larger than that observed one and an interstice of cloud did not occur. HERMAN and GOODY (1976) explained that a separation of the cloud into two cloud layers was due to little diurnal variation of solar radiations and the continuous trapping of the radiation inside a cloud. However, in our calculation the total radiative heating rate is only 0.15°C/hour, which is too small to evaporate the cloud droplets entirely. But, if a thinner cloud is formed, the solar radiation will penetrate more deeply and will be trapped into a lower layer of the cloud, so that the level of maximum heating rate due to absorption of solar radiation will be lowered. On the contrary, the level of maximum cooling rate due to infrared radiation will not change so much. Consequently, the total radiative heating rate will have a greater value at the lower level in the cloud, which will completely evaporate the cloud droplets there.

From these considerations, it seems necessary to investigate more realistic profiles of the temperature and the relative humidity for the initial condition which will give us much plausibly simulated results.

Acknowledgments

The author wishes to express his gratitude for the guidance and encouragement received from Prof. Masayuki TANAKA, Faculty of Science, Tohoku University and Prof. Toshiichi OKITA, Faculty of Engineering, Hokkaido University.

References

BIGNELL, K., SAIEDY, F. and SHEPPARD, P. A. (1963): On the atmospheric infrared continuum. J. Opt. Soc. Am., **53**, 466–479.

BLACKADAR, A. K. (1962): The vertical distribution of wind and turbulent exchange in a neutral atmosphere. J. Geophys. Res., **67**, 3095–3102.

BURCH, D. E. (1970): Investigation of the Absorption of Infrared Radiation by Atmospheric Gases. Semi-annual technical report. AFCRL, Publication U-4784, Contract No. F19628-69-C-0263.

HALE, G. M. and QUERRY, M. R. (1973): Optical constants of water in the 200-nm to 200-μm wavelength region. Appl. Opt., **12**, 555–563.

HANSON, K. J. (1961): The albedo of sea-ice and ice islands in the Arctic Ocean Basin. Arctic, **14**, 188–196.

HERMAN, G. and GOODY, R. (1976): Formation and persistence of summertime arctic stratus clouds. J. Atmos. Sci., **33**, 1537–1553.

JAYAWEERA, K. O. L. F. (1977): The influence of local wind field on the formation of arctic stratus clouds. Proceedings of IAGA/IAMAP Joint Assembly, Seattle, 169.

JAYAWEERA, K. O. L. F. and OHTAKE, T. (1973): Concentration of ice crystals in arctic stratus clouds. J. Rech. Atmos., **7**, 199–207.

JAYAWEERA, K. O. L. F. and OHTAKE, T. (1977): Temperature and emissivity profiles in arctic stratus clouds. Proceedings of IAGA/IAMAP Joint Assembly, Seattle, 170.

KONDO, J. (1975): Air-sea bulk transfer coefficients in diabatic conditions. Boundary-Layer Meteorol., **49**(9), 91–112.

KONDO, J., KANECHIKA, O. and YASUDA, N. (1978): Heat and momentum transfer under strong stability in the atmospheric surface layer. J. Atmos. Sci., **35**, 1012–1021.

OHTA, S. and TANAKA, M. (1981): A numerical study of the formation and dissipation of radiation fog. To be published in J. Meteorol. Soc. Jpn., **59**.

RODGERS, C. D. and WALSHAW, C. D. (1966): The computation of infrared cooling rate in planetary atmospheres. Q. J. R. Meteorol. Soc., **92** 67–92.

SASAMORI, T. (1970): A numerical study of atmospheric and soil boundary layers. J. Atmos. Sci., **27**, 1122–1137.

TANAKA, M. and OHTA, S. (1981): On the method of calculating the radiative transfer by P_3 approximation in foggy and cloudy atmospheres. To be published in J. Quant. Spectrosc. Radiat. Transfer.

VALLEY, S. L. (1965): Handbook of Geophysics and Space Environments. Air Force Cambridge Reseach Laboratories, Office of Aerospace Reseach, U.S. Air Force.

VOWINCKEL, E. and ORVIG, S. (1970): The climate of the north polar basin. Climates of Polar Regions, ed. by S. ORVIG. Amsterdam, Elsevir, 129–252 (World Survey of Climatology, **14**).

YAMAMOTO, G. and SHIMANUKI, A. (1966): Turbulent transfer in diabatic conditions. J. Meteorol. Soc. Jpn, Ser, 2, **44**, 301–307.

ZAKHAROVA, I. M. (1973): Mathematical model of the evolution of radiation fog. Hydrodynamics and Thermodynamics of Aerosols. New York, J. Wiley, 141–159.

ZDUNKOWSKI, W. G. and BARR, A. E. (1972): A radiative-conductive model for the prediction of radiation fog. Boundary-Layer Meteorol., **3**, 152–177.

(Received April 1, 1981; Revised manuscript received May 18, 1981)